

# Monitoring Stem Cell Therapy *in Vivo* Using Magnetodendrimers as a New Class of Cellular MR Contrast Agents<sup>1</sup>

Jeff W. M. Bulte, PhD, Trevor Douglas, PhD, Brian Witwer, MD, Su-Chun Zhang, MD, PhD, Bobbi K. Lewis, BA, Peter van Gelderen, PhD, Holly Zywicke, BS, Ian D. Duncan, BVMS, PhD, FRCVS, FRCPath, Joseph A. Frank, MD

## RATIONALE AND OBJECTIVES

Human embryonic stem (ES) and germ (EG) cells have been isolated and can now be propagated indefinitely in culture (1,2). They can be differentiated into most, if not all cell types, and offer unprecedented therapeutic potential to replace or substitute defunct endogenous cell populations. In order to track the biodistribution of transplanted cells in animals, including their migration *in vivo*, cells can be given a tag before grafting. These tags currently include fluorescent labels, thymidine analogues, and transfected reporter genes (e.g. LacZ or GFP), which can be visualized using (immuno)histochemical procedures following tissue removal at a particular given time point. The clinical use of progenitor and stem cells in humans, however, will require a technique that can monitor their fate non-invasively and repeatedly, in order to take a momentary “snapshot” assessment of the cellular biodistribution at a particular given time point. As a result, magnetic resonance (MR) tracking of magnetically labeled stem and progenitor cells is now emerging as a new technology (3,4). A further implementation of this potentially powerful technique will greatly benefit from the

availability of magnetic probes that can render cells highly magnetic during their normal expansion in culture (5).

We present here magnetodendrimers (MD-100) as a new class of magnetic probes that can achieve a high degree of intracellular magnetic labeling for virtually any cell type, including human mesenchymal and neural stem cells (NSCs). Our rationale to use dendrimers as the iron oxide-associated polymer is based upon its reported high efficiency to shuttle other macromolecules such as oligonucleotides across cell membranes (7). Analogous to the use of dendrimers as transfection agents (including the commercially available agents Superfect™ and Polyfect™), a key feature of magnetodendrimers is its universal applicability for the magnetic labeling of cells, that is, the cellular uptake is non-specific and not dependent on binding to membrane receptors. Using a rat brain transplantation model, we show here that NSC-derived, MD-100-labeled oligodendroglial progenitors can be readily detected *in vivo* following transplantation, with an excellent correlation between the obtained MR contrast and staining for (LacZ) transfected  $\beta$ -galactosidase.

## MATERIALS AND METHODS

A general scheme for the synthesis of soluble iron oxide-dendrimer composites has been published recently (6). Briefly, to obtain MD-100, carboxyl-terminated dendrimers ( $G = 4.5$ , Dendritech, Midland, MI) were incubated, under anaerobic conditions, with  $(\text{NH}_4)_2\text{Fe}(\text{SO}_4)_2 \cdot 6\text{H}_2\text{O}$  at a loading factor of 100 iron atoms per molecule. The mixture was then oxidized with the 2-electron oxidant  $\text{Me}_3\text{NO}$  to yield a homogeneous brown solution, and was

Acad Radiol 2002; 9(suppl 2):S332-S335

<sup>1</sup> From the Laboratory of Diagnostic Radiology Research (CC) (J.W.M.B., B.K.L., H.Z., J.A.F.) and Functional and Molecular Imaging (NINDS) National Institutes of Health, Bethesda, MD(P.G.); Dept. of Chemistry, Temple University, Philadelphia, PA(T.D.); Department of Medical Sciences, School of Veterinary Medicine, University of Wisconsin, Madison, WI(B.W., S.Z., I.D.D.). Address correspondence to J.W.M.B. Dept Radiol, Johns Hopkins Univ School of Med, 217 Taylor Bldg, 720 Rutland Ave, Baltimore, MD 21205-2195.

© AUR, 2002

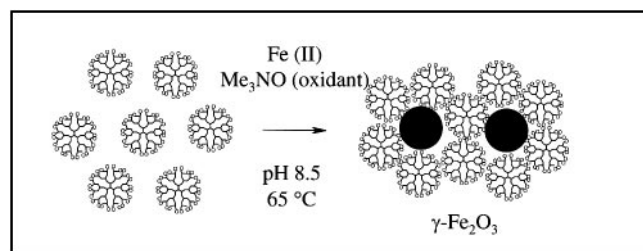


**Figure 1.** Schematic representation of the stabilization of maghemite nanoparticles by carboxyl-terminated poly(amido-amine) dendrimer. For simplicity, a G = 3 dendrimer is shown; a G = 4.5 dendrimer was used in the actual synthesis.

further purified before use. Physicochemical characterization of the obtained preparations included size exclusion chromatography and electron microscopy. For NMR relaxometry, MD-100 samples were measured using a custom-designed variable-field relaxometer at temperatures of 3 and 37 °C. For T1, 32 saturation-recovery sequences were used; T2 was measured with a CPMG sequence of 500 echoes with interecho time TE = 2 ms. The range of field strengths was 0.05-1.5 Tesla.

Mammalian cells (human neural stem cells (NSC), human mesenchymal stem cells (MSC), human HeLa cervix carcinoma, human GLC-28 small cell lung carcinoma, rat NSC, rat CG-4 oligodendrocyte progenitors, mouse NIH 3T3 fibroblasts, mouse C2C12 muscle progenitors) were co-cultured for 24-48 h in standard media containing MD-100 at a dose ranging from 1 to 25  $\mu\text{g}$  Fe/ml. NSCs were allowed to differentiate into neurons and glial cells by withdrawal of growth factors. For assessment of toxicity and normal proliferation of MD-100 labeled cells, cells were tested in an MTT (3-[4,5-dimethylthiazol-2-yl]-2,5-diphenyl tetrazolium bromide) assay. All cells were trypsinized and washed three times for further analysis. This included (DAB-enhanced) Prussian Blue staining, T1 and T2 relaxometry at 0.1 and 1.0 Tesla, and MR imaging of labeled cell pellets. The relaxometry was further correlated to the amount of internalized MD-100 using an acid digestion/spectrophotometric iron assay.

In vivo animal experiments were conducted in accordance with institutional guidelines for the use and care of laboratory animals. Rat oligodendroglial progenitors (oligospheres) were prepared from NSC as described (9), transfected with the LacZ reporter gene, trituated, and labeled with MD-100 for 24h at 25  $\mu\text{g}$  Fe/ml. Approximately  $5 \times 10^4$  cells in 2-3  $\mu\text{l}$  medium were transplanted into both lateral intracerebroventricular regions of neonatal (P0) *les* rats (n=5). Under general isoflurane anesthe-

sia, pups were imaged at 1.5 T (Signa, GE) at 18, 25, 31, and 44 days post grafting, using a quadrature wrist coil and several different clinical pulse sequences, including T1-weighted (w), T2-w, proton density, FSE, and GRE 2D images, obtained at 2 mm slice thickness. A 3D SPGR data set was also obtained using a slice thickness of 1.2 mm. In addition, at 21 and 42 days post grafting, 3D multi-gradient echo MR images were obtained at 313  $\mu\text{m}$  isotropic resolution using a 4.7 T Varian Inova NMR spectrometer and a 1.5 inch diameter home-made surface coil. The latter parameters were: FOV =  $4 \times 3 \times 3$  cm; matrix =  $128 \times 96 \times 96$ ; NEX = 1; TR = 100 msec; TE = 6 msec; n echoes = 6, flip angle = 15 deg. Following imaging, paraformaldehyde-perfused brain specimens were cut into 2 mm slices for gross morphology and stained with X-gal for  $\beta$ -galactosidase (LacZ) expression.

## RESULTS

Electron microscopic assessment of the MD-100 preparations revealed an oligocrystalline structure of 7-8 nm crystals separated by a somewhat smaller distance. Since the diameter of a G = 4.5 dendrimer is approximately 5 nm, we propose the actual structure to resemble that of Figure 1. This result is different from the initial reports (10-12) describing the presence of intradendritic metal particles but is consistent with a later report (13) in which the mineral particles are not entrapped within the dendrimer but grow from the dendrimer surface. The measured T1 relaxivities dropped exponentially from 138-94 at 0.05 Tesla to 11-7  $\text{mM}^{-1} \text{s}^{-1}$  at 1.5 Tesla for 3 and 37 °C, respectively. On the other hand, the measured T2 relaxivities demonstrated near saturation at the lowest field measured (0.05 Tesla), with unusually high values of 200-406  $\text{mM}^{-1} \text{s}^{-1}$  (at 3 and 37 °C, respectively). Prussian Blue staining of magnetically tagged cells showed a remarkable high degree of intracellular labeling, with the cytoplasm containing large numbers of iron-containing vesicles or endosomes (Figure 2). All cells showed a comparable degree of uptake, demonstrating that the MD-100 uptake is non-specific and not dependent on the cell type or species. Cells remained fully viable with no difference in growth and proliferation between labeled and unlabeled cells. The 1/T1 of labeled cell suspensions showed a significant increase as compared to non-labeled controls but was small as compared to the dramatic increase of 1/T2, which was up to 50-150  $\text{s}^{-1}$  depending on cell density. The cellular uptake was calculated to be between 9 and 14 pg Fe per cell. The "cellular relaxivity"

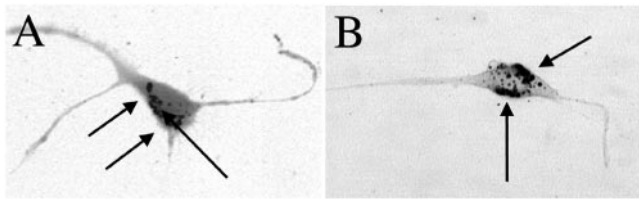


**Figure 2.** (a) Non-enhanced and (b) DAB-enhanced Prussian Blue stains of MD-100 labeled, NSC-derived oligodendroglial precursor cells shows the presence of numerous iron-containing vesicles in the cytoplasm.

(i.e. increase in cellular relaxation rates per unit Fe concentration) was between 1.8 and 2.6  $s^{-1}mM^{-1}$  Fe at either low or high field. The cellular T2 relaxivity was calculated to be between 47.0 and 78  $s^{-1}mM^{-1}$  Fe. These values indicate a near 50-fold reduction in T1 relaxivity for MD-100 when going from an unbound, free-in-solution state to a state representing intracellular compartmentalization in endosomes. This most likely reflects the less rapid inner-sphere exchange of water molecules inside the cell as well as a reduced molecular exchange with bulk water through a “membrane shielding” effect. On the other hand, the cellular T2 relaxivity decreases only about 5-fold because there can be a significant remaining outer-sphere relaxation effect for dipole-dipole or spin-spin type interactions that does not contribute to  $1/T_1$ , in addition to dephasing and T2\* susceptibility effects (which were kept small by the short interecho time of refocusing  $180^\circ$  pulses that was used in the CPMG experiments); the overall result is a net increase in the  $1/T_2$  to  $1/T_1$  ratio.

Human NSCs and MSCs could be highly labeled with MD-100 at doses of only 1–2.5  $\mu g$  Fe/ml. They exhibited a similar growth rate as unlabeled cells, and NSCs showed a comparable formation of neuronal processes when replated and grown for an additional 10 days. Morphologically, labeled NSC resembled differentiation into glial cells and neurons, as demonstrated by immunospecific staining using neuronal markers. We then assessed the possibility of detecting MD-100 labeled cells *in vivo*. Rat NSCs were differentiated into oligodendroglial progenitors, transfected with the LacZ gene, labeled with MD-100, and injected into both lateral ventricles of neonatal (P0) Long Evans shaker (*les*) rats. These animals are dysmyelinated mutants resulting from a defect in the gene encoding for myelin basic protein (14). Animals were imaged at weekly to biweekly intervals to determine the tissue distribution of transplanted cells. Fig. 3A shows an MR image obtained *in vivo* using a 4.7 Tesla animal MR imaging unit 6 weeks post transplantation. Migration

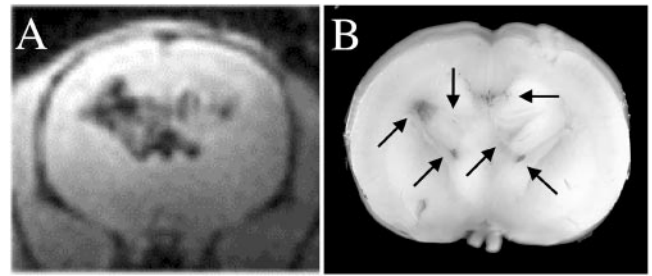


**Figure 3.** (a) *In vivo* MR image (0.3 mm in-plane resolution) of a *les* rat 42 days post intraventricular transplantation of MD-100 labeled and LacZ-transfected, NSC-derived oligodendroglial progenitors. (b) Despite any partial volume averaging effect, note the close overlap between the MR contrast and the X-gal staining of the corresponding gross specimen (arrows).

of labeled cells into the brain parenchyma can be clearly detected, with a good anatomical correlation with the macroscopic distribution of  $\beta$ -galactosidase-expressing cells (Fig. 3B). Note that the area of MR contrast appears to spread somewhat further into the brain parenchyma; this is partially related to the fact that we used a T2\*-sensitive 3D imaging sequence that is very sensitive to MD-100-induced local disturbances in the magnetic field. This causes water protons at more remote sites to be affected as well, leading to a “blooming effect”, i.e. an amplification of signal changes. MD-100 labeled cells could also be readily identified *in vivo* using a conventional 1.5 Tesla clinical imaging system (results not shown), suggesting that our approach may indeed be useful to help guide future advances in human stem cell-based therapies.

## CONCLUSION

Based upon the use of dendrimers as transfection agents, magnetodendrimers represent a new type of superparamagnetic probes that have desirable magnetic relaxation properties and that show a high, non-specific affinity for cellular membranes. These novel nanoparticles allow intracellular magnetic labeling of mammalian (stem) cells regardless of their origin or animal species, opening up the possibility of MR tracking of a wide variety of cell transplants.

## REFERENCES

1. Thomson JA, et al. Embryonic stem cell lines derived from human blastocysts. *Science* 1998; 282:1145–1147.
2. Shambloott MJ, et al. Derivation of pluripotent stem cells from cultured human primordial germ cells. *Proc Natl Acad Sci USA* 1998; 95:13726–13731.

3. Bulte JWM, et al. Neurotransplantation of magnetically labeled oligodendrocyte progenitors: MR tracking of cell migration and myelination. *Proc Natl Acad Sci USA* 1999; 96:15256–15261.
4. Lewin M, et al. Tat peptide-derivatized magnetic nanoparticles allow in vivo tracking and recovery of progenitor cells. *Nature Biotechnol* 2000; 18:410–414.
5. Bulte JWM, Bryant LH. Molecular and cellular magnetic resonance contrast agents. In: *Focus on Biotechnology, Vol. 7* (de Cuyper, M. & Bulte, JWM, Eds), Kluwer Academic Press, 2001; 197–211.
6. Strable E, Bulte JWM, Moskowitz B, Vivekanandan K, Douglas T. Synthesis and characterization of soluble iron oxide-dendrimer composites. *Chem Mater* 2001; 13:2201–2209.
7. Kukowska-Latallo JF, Bielinska AU, Johnson J, Spindler R, Tomalia DA, Baker Jr, JA. Efficient transfer of genetic material into mammalian cells using Starburst polyamidoamine dendrimers. *Proc Natl Acad Sci USA* 1996; 93:4897–4902.
8. Tang MX, Redemann CT, Szoka FC. In vitro gene delivery by de-graded polyamidoamine dendrimers. *Bioconj Chem* 1996; 7:703–714.
9. Zhang S-C, Lundberg C, Lipsitz D, O'Connor LT, Duncan ID. Generation of oligodendroglial progenitors from neural stem cells. *J Neurocytol* 1998; 27:475–489.
10. Zhao MQ, Sun L, Crooks RM. Preparation of Cu nanoclusters within dendrimer templates. *J Am Chem Soc* 1998; 120:4877–4878.
11. Balogh L, Tomalia DA. Poly(amidoamine) dendrimer-templated nanocomposites. 1. Synthesis of zerovalent copper nanoclusters. *J Am Chem Soc* 1998; 120:7355–7356.
12. Zhao MQ, Crooks RM. Homogeneous hydrogenation catalysis with monodisperse, dendrimer-encapsulated Pd and Pt nanoparticles. *Angew Chem Int Ed* 1999; 38:364–366.
13. Garcia ME, Baker LA, Crooks RM. Preparation and characterization of dendrimer-gold colloid nanocomposites. *Anal Chem* 1999; 71:256–258.
14. O'Connor LT, Goetz BD, Kwiecien JM, Delaney KH, Fletch AL, Duncan ID. Insertion of a retrotransposon into the Mbp disrupts mRNA splicing and myelination in a new mutant rat. *J Neurosci* 1999; 19:3404–3413.